

## Azimuthal AVO inversion by simulated annealing

David Cho and Gary F. Margrave

### ABSTRACT

Fractures influence the permeability pathways and mechanical properties associated with a rock mass and therefore, are a crucial aspect in the characterization of the subsurface. In this study we develop an azimuthal AVO inversion algorithm using a simulated annealing optimization technique. The parameterization of the problem is in terms of an isotropic background with the inclusion of fractures through an addition of excess compliances to the medium. Preliminary inversion results demonstrate a reasonable estimate of the model parameters in addition to an excellent match between the data and synthetic data. Associated errors in the estimated model parameters are attributed to variable sensitivities of the model parameters to the objective function. Future work will attempt to address these issues through different parameterizations of the problem and additional constraints in the objective function.

### INTRODUCTION

Characterization of azimuthally anisotropic media has been the subject of considerable interest in recent years, where the observed anisotropy could indicate the presence of oriented fractures in the subsurface. Fractures influence the permeability pathways and alter the mechanical properties of the rock mass, where they weaken or perhaps even strengthen its structure in prescribed directions. In addition, anisotropic materials result in differential stresses upon loading and result in deviations from the regional stress field. Knowledge of anisotropic parameters is therefore crucial in the characterization of the subsurface.

In this study, we develop an azimuthal AVO inversion algorithm to estimate subsurface anisotropic parameters from reflection seismic measurements. The approach is similar to that of Downton and Roure (2010) where a fracture model is used for the parameterization of the problem. Beginning with a set of initial model parameters, a synthetic dataset is generated using a forward modeling scheme and the system is subsequently optimized to obtain a solution that minimizes a defined objective function.

### FORWARD MODEL

The objective of an inverse problem is to obtain a set of model parameters (elastic properties) that reproduce the associated observations or data (seismic measurements) that correspond to some physical process (reflection from an interface). The forward problem is represented by

$$Gm = d \tag{1}$$

where  $G$  represents the forward operator,  $m$  is the set of model parameters and  $d$  is the data.

In the formulation of the forward problem, we assume an Earth model consisting of transversely isotropic (TI) layers, where the transverse isotropy is due to the presence of an aligned fracture system as shown in Figure 1.

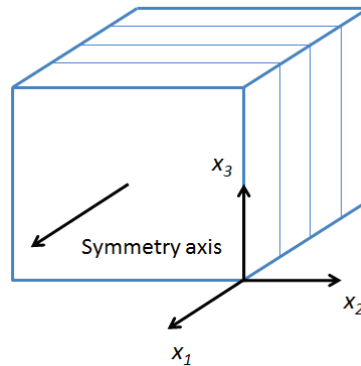


FIG. 1. TI medium with a symmetry axis that coincides with the  $x_1$  axis.

Beginning with an isotropic background medium defined by the Lamé parameters,  $\lambda$  and  $\mu$  and density, we use the linear slip deformation model of Schoenberg and Sayers (1995) to insert fractures through the addition of a normal,  $Z_N$  and tangential,  $Z_T$  fracture compliance to the isotropic fourth rank elastic compliance tensor. Subsequently, the inverse is calculated to obtain the effective elastic stiffness tensor for a medium containing fractures. In addition, a coordinate rotation about the  $x_3$  axis can be performed using Bond (1943) transformations to represent various fracture azimuths. The parameterization of the problem is therefore in terms of  $\lambda$ ,  $\mu$ , density, normal and tangential fracture compliance and fracture azimuth.

A TI medium is represented by nine non-vanishing elastic stiffness parameters when its symmetry axis coincides with one of the coordinate axes. When this is not the case, additional parameters appear in the elastic stiffness tensor and the medium cannot be regarded as a TI medium in the given coordinate system. Therefore, in calculating the reflection coefficients, simpler formulations such as that of Rüger (1998) for a TI media with a horizontal axis of symmetry (HTI) is insufficient. Here we use the formulation of Vavryčuk and Pšenčík (1998), which provides the P-wave reflection coefficients for weak contrast interfaces separating two weakly but arbitrarily anisotropic media. The derivation was based on a perturbative analysis, therefore requires the definition of a background P- and S-wave velocity. Here, the background P- and S-wave velocities were chosen to be the vertical P-wave velocity and the vertical S-wave velocity with a polarization in the  $x_2$ - $x_3$  plane. The P-wave reflection coefficient is then given by

$$\begin{aligned}
R_{PP}(\theta, \phi) = & R_{PP}^{iso}(\theta) + \frac{1}{2} \left[ \Delta \left( \frac{A_{23} + 2A_{44} - A_{33}}{A_{33}} \right) \sin^2 \phi \right. \\
& + \left( \Delta \left( \frac{A_{13} + 2A_{55} - A_{33}}{A_{33}} \right) - 8\Delta \left( \frac{A_{55} - A_{44}}{2A_{33}} \right) \right) \cos^2 \phi \\
& + 2 \left( \Delta \left( \frac{A_{36} - A_{45}}{A_{33}} \right) - 4\Delta \left( \frac{A_{45}}{A_{33}} \right) \right) \cos \phi \sin \phi \left. \right] \sin^2 \theta \\
& + \frac{1}{2} \left[ \Delta \left( \frac{A_{11} - A_{33}}{2A_{33}} \right) \cos^4 \phi + \Delta \left( \frac{A_{22} - A_{33}}{2A_{33}} \right) \sin^4 \phi \right. \\
& + \Delta \left( \frac{A_{12} + 2A_{66} - A_{33}}{A_{33}} \right) \cos^2 \phi \sin^2 \phi + 2\Delta \left( \frac{A_{16}}{A_{33}} \right) \cos^3 \phi \sin \phi \\
& \left. + 2\Delta \left( \frac{A_{26}}{A_{33}} \right) \sin^3 \phi \cos \phi \right] \sin^2 \theta \tan^2 \theta
\end{aligned} \tag{2}$$

and

$$R_{PP}^{iso}(\theta) = \frac{1}{2} \frac{\Delta Z}{\bar{Z}} + \frac{1}{2} \left[ \frac{\Delta \alpha}{\alpha} - \left( \frac{2\bar{\beta}}{\alpha} \right)^2 \frac{\Delta G}{G} \right] \sin^2 \theta + \frac{1}{2} \frac{\Delta \alpha}{\alpha} \sin^2 \theta \tan^2 \theta, \tag{3}$$

where  $A_{ij}$  represent the density normalized elastic stiffness parameters in Voigt notation with  $i$  and  $j$  running from 1 to 6,  $\alpha$  and  $\beta$  are the background P- and S-wave velocities respectively,  $Z = \rho\alpha$  is the acoustic impedance,  $G = \rho\beta^2$  is the shear modulus,  $\rho$  is the density,  $\theta$  is the average angle of incidence and  $\phi$  is the measurement azimuth. The bar represents an averaging of the values (i.e.  $\bar{w} = 1/2[w_2 + w_1]$ ) and  $\Delta$  represents a difference of the values (i.e.  $\Delta w = w_2 - w_1$ ) above and below the reflecting interface. Upon calculation of the reflection coefficients, the synthetic seismograms are generated by convolving the reflectivity series with a wavelet.

### SIMULATED ANNEALING

Due to the non-linearity of the forward model as outlined above, an iterative scheme is required to perform the inversion where an initial model is updated iteratively to obtain an optimal solution. Here we use the simulated annealing algorithm which models a physical process in which a solid is slowly cooled until it reaches a state that minimizes its internal energy. The original Metropolis algorithm (Metropolis et al., 1953) that describes the simulated annealing process involves a random walk in the model or solution space. At each step, an energy, which is defined as an error or objective function is calculate for the randomly selected solution. The acceptance criterion is then defined by a change in energy,  $\Delta E < 0$ . However, if  $\Delta E > 0$ , a new solution is accepted with a probability  $\exp(-\Delta E/T)$ , where  $T$  is the temperature of the system.  $T$  is slowly lowered throughout the execution of the algorithm and the system eventually reaches a state of equilibrium or the final solution. The optimal solution is therefore achieved through the

minimization of the objective function. Simulated annealing is in the class of global optimization algorithms that attempt to locate the global minimum of a given function. However, convergence is only guaranteed for a high initial temperature and very slow cooling, which requires enormous compute times. Therefore, the annealing schedule becomes a crucial aspect of the inversion process.

Here we use an alternative implementation of the algorithm as presented by Rothman (1986), which computes the probability of acceptance before a solution is selected. For a given model parameter, the energy is computed for every value within an allowable search range while keeping all other parameters constant. Subsequently, the Gibbs probability density function is calculated using

$$P(m_{ij}) = \frac{\exp(-E(m_{ij})/T)}{\sum_j \exp(-E(m_{ij})/T)}, \quad (4)$$

where the subscript  $i$  represents the model parameters and the subscript  $j$  represents the range of values the model parameter,  $m_i$  can take. A sample is then drawn from the distribution and retained as the new solution for  $m_i$ . This procedure is repeated for all model parameters and represents one iteration. The algorithm then takes the system through subsequent iterations where  $T$  is lowered according to a defined annealing schedule.

In this study, we use a two term energy or objective function defined by

$$E(m_i) = \sum_i (Gm_i - d)^2 + \sum_k w_k \sum_i \left(1 - m_i / m_i^{(initial)}\right)^2, \quad (5)$$

where  $w_k$  is a weight applied to the  $k^{th}$  elastic property and  $m_i^{(initial)}$  represents the initial model used. The first term represents an  $L_2$  norm of the data residuals and the second term controls the deviation from the initial model.

## PRELIMINARY RESULTS

The data used in the inversion was generated using the forward model as discussed above. A two layered Earth model was created where the top layer is isotropic and the bottom layer has a set of vertical fractures. An initial temperature,  $T_0$  was chosen to be 0.05 with an annealing schedule defined by  $T_n = T_0 * 0.6^n$ , where  $n$  represents the iteration number. The initial testing was performed using 20 iterations. Figure 2 shows the Gibbs probability density functions for the model parameters of the top layer after 5, 10 and 15 iterations. Note that the width of the distribution narrows as the temperature decreases with each iteration, converging to a final solution. However, the rate at which the distributions narrow are different for the various model parameters, where  $\lambda$ ,  $\mu$  and density converge at a much faster rate than the normal and tangential fracture compliances and fracture azimuth. Future work will attempt to normalize the convergence rate of each model parameter to optimize the compute time.

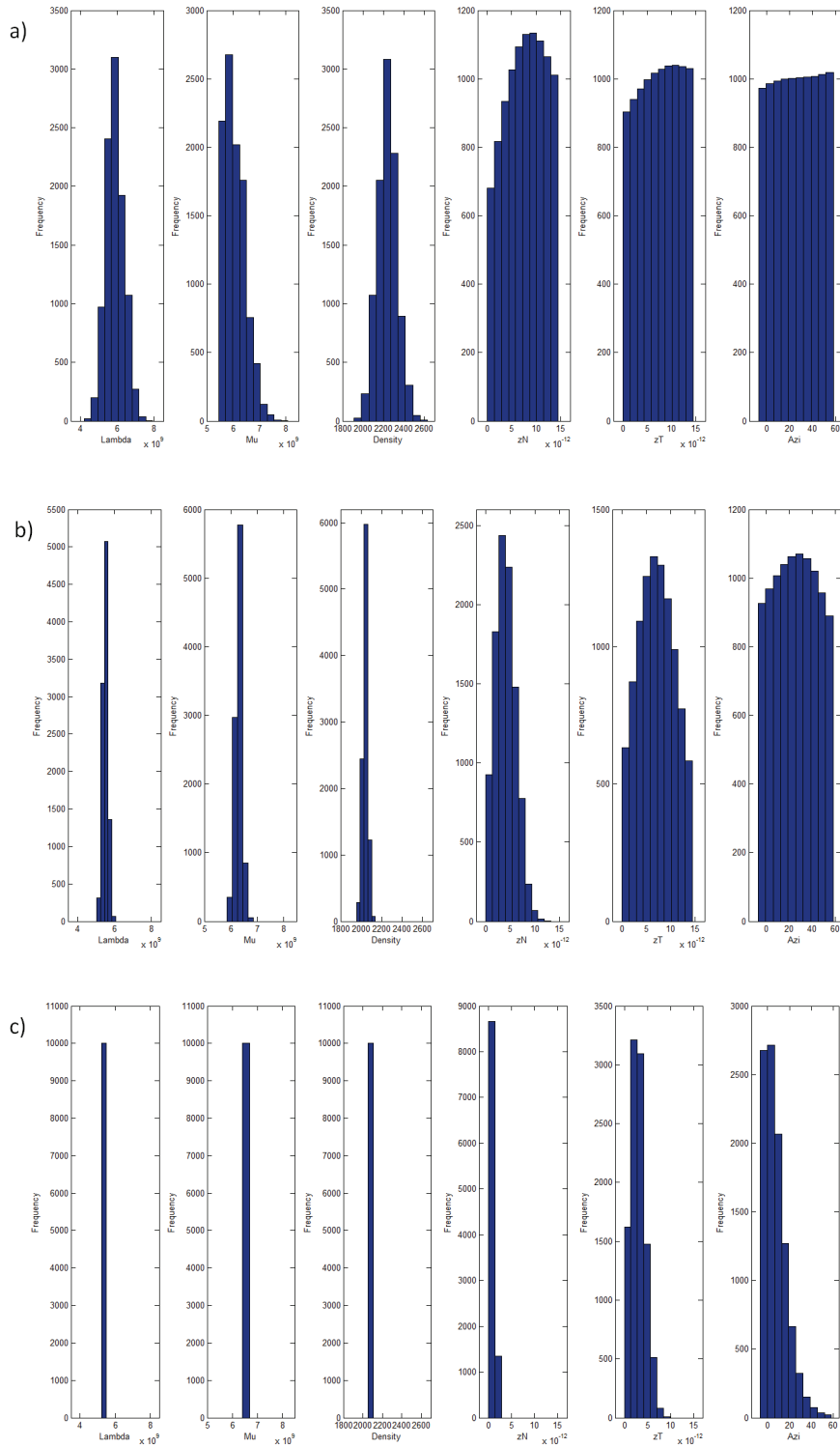


FIG. 2. Gibbs probability density functions for the model parameters of the top layer after a) 5 iterations, b) 10 iterations and c) 15 iterations.

Figure 3 shows the data, synthetic data and the residuals associated with the inversion. The synthetic data demonstrates an excellent match to the data, suggesting that the

inversion algorithm is capable of performing the intended task of minimizing the data residuals.

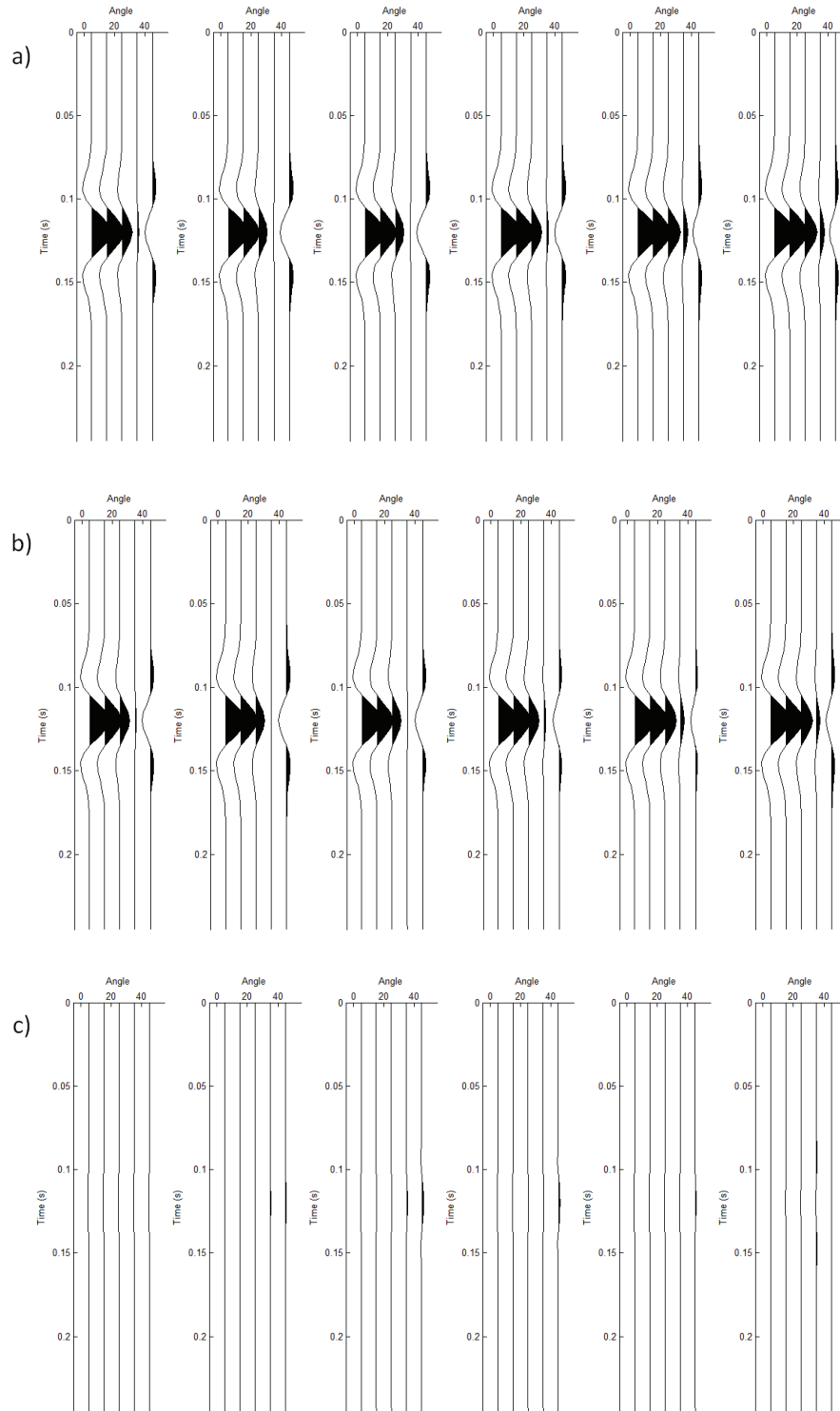


FIG. 3. Azimuthal angle gathers representing the a) data, b) synthetic data and c) residuals associated with the inversion. Each panel represents a single azimuth of 30, 60, 90, 120 and 150 degrees from left to right.

Figure 4 shows the inversion results along with the true model and the initial model used. The preliminary results demonstrate a reasonable estimate of the model parameters where the errors are different amongst the various parameters. Since the residuals are small as shown in Figure 3, the errors are attributed to the parameterization of the problem where the sensitivity of the model parameters to the objective function is variable. Future work will explore different parameterizations and additional constraints in the objective function to optimize the inversion results.

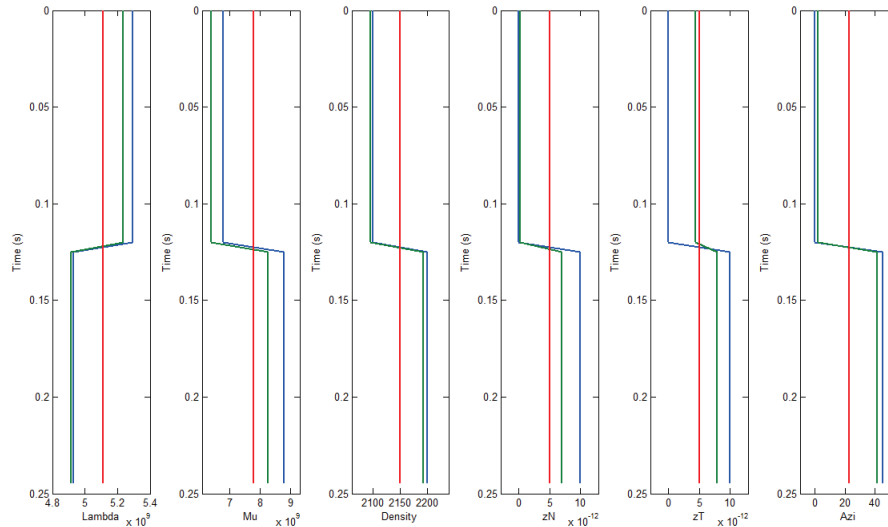


FIG. 4. Results showing the true model (blue), initial model (red) and inverted model (green).

## CONCLUSIONS

An azimuthal AVO inversion was performed using a simulated annealing technique. The preliminary results demonstrate a reasonable estimate of the model parameters in addition to an excellent match between the data and synthetic data. The associated errors are then attributed to the parameterization of the problem where the sensitivity to the objective function of each model parameter varies. Future work will explore alternative parameterizations and constraints in the objective function to optimize the inversion.

## ACKNOWLEDGEMENTS

Many thanks to Faranak Mahmoudian for insightful discussions on the topic of anisotropy and the sponsors of the CREWES project.

## REFERENCES

- Bond, W., 1943, The mathematics of the physical properties of crystals: *BSTJ*, 22, 1-72.
- Downton, J., Roure, B., 2010, Azimuthal simultaneous elastic inversion for fracture detection: 80th Annual International Meeting, SEG, Expanded Abstracts, 263-267.
- Metropolis, N., Rosenbluth, A., Rosenbluth, M., Teller, A., and Teller, E., 1953, Equation of state calculations by fast computing machines: *J. Chem. Phys.*, 21, 1087-1092.
- Rothman, D. H., 1985, Nonlinear inversion, statistical mechanics and residual statics estimation: *Geophysics*, 50, 2784-2796.
- Rüger, A., 1998, Variation of P-wave reflectivity with offset and azimuth in anisotropic media: *Geophysics*, vol. 63, no. 3, P. 935-947.

Schoenberg, M., and C. Sayers, 1995, Seismic anisotropy of fractured rock: *Geophysics*, 60, 204–211.

Vavryčuk, V., Pšenčík, I., 1998, PP-wave reflection coefficients in weakly anisotropic elastic media: *Geophysics*, vol. 63, no. 6, P. 2129-2141.